
# UV and fluorescent spectra study the reaction between 1, 8-Naphthalimide derivative and hypochlorite their applications

Jiawei Li, Tao Liu, Fangjun Huo, Jianbin Chao, Yongbin Zhang, Caixia Yin

PII: S1386-1425(16)30673-4
DOI: doi:10.1016/j.saa.2016.11.019
Reference: SAA 14779

To appear in:

Received date: 20 August 2016
Revised date: 2 November 2016
Accepted date: 13 November 2016

Please cite this article as: Jiawei Li, Tao Liu, Fangjun Huo, Jianbin Chao, Yongbin Zhang, Caixia Yin, UV and fluorescent spectra study the reaction between 1, 8-Naphthalimide derivative and hypochlorite their applications, (2016), doi:10.1016/j.saa.2016.11.019

# UV and fluorescent spectra study the reaction between 1, 8-Naphthalimide derivative and hypochlorite their applications

§ Jiawei Li [a], § Tao Liu,[a] Fangjun Huo[b,*], Jianbin Chao[b], Yongbin Zhang[b], Caixia Yin [a,**]

[a]Key Laboratory of Chemical Biology and Molecular Engineering of Ministry of Education, Key Laboratory of Materials for Energy Conversion and Storage of Shanxi Province, Institute of Molecular Science, Shanxi University, Taiyuan, 030006, China;[b]Research Institute of Applied Chemistry, Shanxi University, Taiyuan, 030006, China.

*Corresponding author: C.X. Yin, E-mail: yincx@sxu.edu.cn;

**Corresponding author: F.J. Huo, Email: huofj@sxu.edu.cn.

§Jiawei Li and Tao Liu contributed equally

**Abstract:** Two simple, efficient turn-on fluorescent probes for hypochlorite have been rationally designed and developed by utilizing the oxidation of hypochlorite. Notably, probe **1** and **2** displayed rapid and remarkable turn-on responses to $ClO^-$ in PBS buffer solution (pH 7.4). Further, the optical properties of two probes and their $ClO^-$-addition products were confirmed by density functional theory calculations. And detection limits of two probes for $ClO^-$ based on the definition by IUPAC were calculated for 2.882 nM and 0.354 μM. More importantly, cell imaging experiments demonstrated that probe **1** was more suitable for detecting the $ClO^-$ in living A549 cells. And both two probes had the possibility of potentially applied in practical applications such as detecting the hypochlorite concentration of tap water and river water.

*Keywords:* Turn-on; Fluorescent probes; Hypochlorite; Theory calculations; Cell imaging

## 1. Introduction

A series of reactive oxygen species (ROS) can be produced in the normal physiological metabolism of aerobic cells, which play an indispensable role in the metabolism of organisms and have a pivotal influence on the process of life.[1-3] ROS at a normal level are conducive to control and regulate a wide range of physiological functions, but abnormal content of ROS can results in oxidative stress which are connected with the pathogenesis of many diseases.[4,5] Hypochlorous acid (HOCl) and its conjugate base hypochlorite ($ClO^-$) are one type of important ROS. In living organisms, the endogenous hypochlorite can be produced by peroxidation of chloride ions catalyzed the enzyme myeloperoxidase (MPO).[6,7] As important signaling molecules, they can control and mediate a wide range of physiological and biological process, such as control of cell life cycle, reparation of tissue as well as antimicrobial activity in the defense system. Hypochlorite has an important antimicrobial effect in living body, thus endogenous hypochlorite is very necessary for life. However, excess concentration of hypochlorite can be implicated in many tissue damages and a variety of human diseases, such as rheumatoid,[8] cardiovascular diseases,[9] lung injury,[10] hepatic ischemia-reperfusion injury,[11] atherosclerosis,[12] neuron degeneration[13] and even cancer.[14] Additionally, hypochlorite is indispensable and essential for our daily life, which can be often used as bleach, deodorant and disinfectant. Also, it is widely used as a bleacher in paper pulp and textiles, a disinfectant in drinking water, milk industries, a purifying treatment in swimming pool water, wastewater, cooling water and a disinfectant agent in hospital and daily life and so on.[15,16] As a chlorinated

disinfectant, its disinfection effect is done by the generation of hypochlorite. But when hypochlorite as a chlorinated disinfectant is used, this process will produce chlorate or chlorite, they have potential hazards to the human body.[17] Thus all countries in the world have already stipulated the use of the highest hypochlorite concentration in drinking water. And our country has stipulated that hypochlorite is handled as concentrated aqueous solutions, typically, in the concentration range of $10^{-5}$ to $10^{-2}$ M, [18] which is a potential health hazard to human and animals.[19]

Therefore, to build and develop high efficient, selective and sensitive methods for direct detection of $ClO^-$ in environmental and other fields are of considerable importance. Compared with traditional detection methods, fluorescent probes have innate advantages including efficient selectivity, better sensitivity and quick response time, some of which be allowed be used to monitor analyte at physiological levels in vitro and in vivo. [20-23] Based on different fluorophores, fluorescent probes have been developed based on coumarin, fluorescein, rhodamine, 1, 8-naphthalimide, BODIPY and so on.[24-28]

Generally speaking, 1, 8-naphthalimide type fluorescent materials are application of a very wide range of important functional materials. From the molecular structure, this kind of compound molecules have a rigid and good planarity naphthalene ring structure unit, and it itself contains a strong electron acceptor and an electron donor and exists an intramolecular charge transfer (ICT) process, so it has good photoluminescence and electroluminescence properties. Because of these fascinating and excellent properties such as high quantum yields, good photostability and large

stokes shift, 1, 8-naphthalimide-based derivatives have been widely used in fluorescence detection and imaging. By utilizing the virtue of its specific features, we design and synthesized two simple, efficient 1, 8-naphthalimide-based fluorescent probes for detecting $ClO^-$, which feature excellent selectivity and high sensitivity for $ClO^-$ over other analytes (Scheme 1).

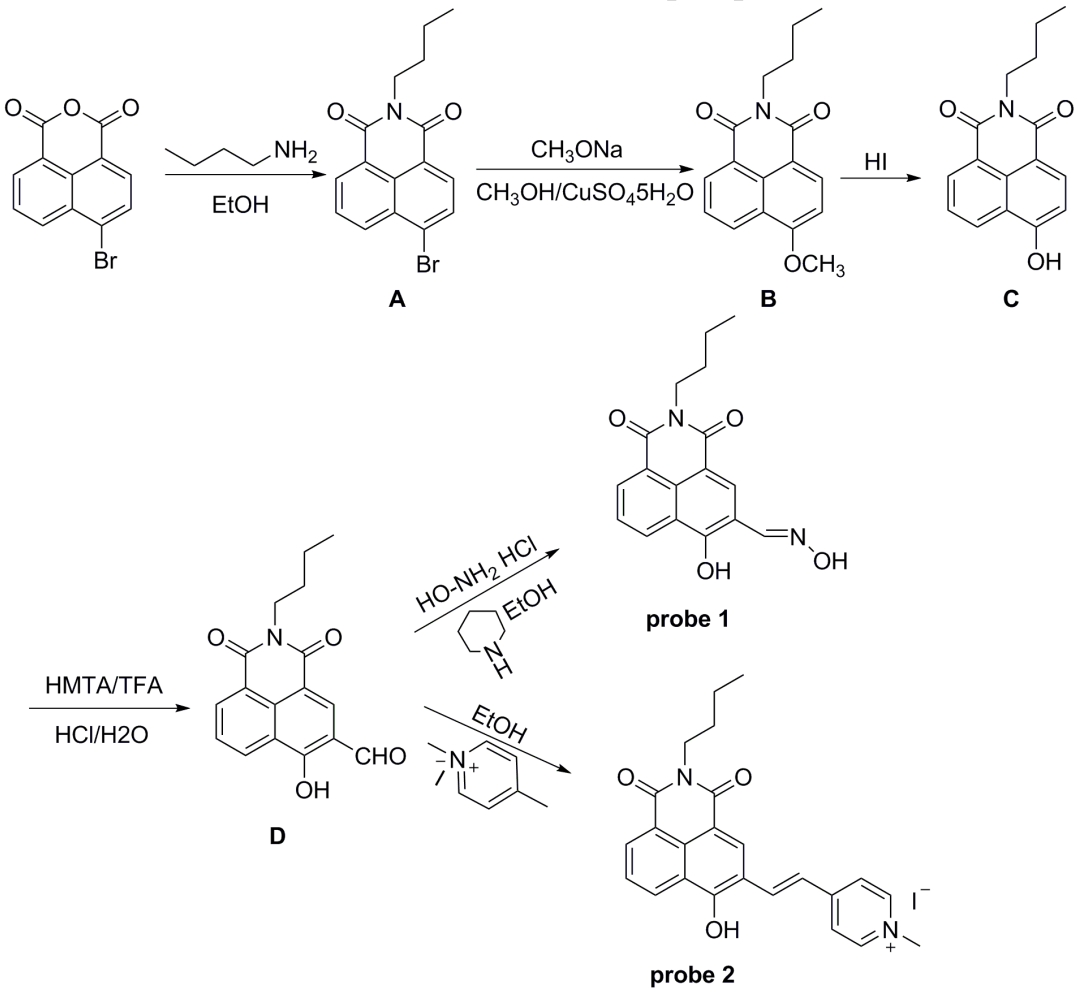


**Scheme 1** Synthesis of probe **1** and **2**.

## 2. Experimental

### *2.1 Materials*

Unless otherwise stated, all reagents and analytes were purchased from commercial suppliers and were of analytical grade without further purification. $H_2O$ was deionized

and was used throughout all experiments. The solutions of anions were prepared from their sodium salts, respectively. The spectroscopic measurements of probe **1** and **2** were performed in PBS buffer solution (pH 7.4) and PBS buffer solution (pH 7.4, containing 20% DMSO), respectively.

*2.2. Instruments*

A pH meter (Mettler Toledo, Switzerland) was used to determine the pH. Reactions were carried out on the magnetic stirrers and their reaction processes were monitored on thin layer chromatography (TLC). UV-Vis spectra and fluorescence spectra were measured on a Cary 50 Bio UV-Visible spectrophotometer and a Hitachi F-7000 fluorescence spectrophotometer, respectively. A PO-120 quartz cuvette (10 mm) was purchased from Shanhai Huamei Experiment Instrrument Plants, China. $^{1}$H NMR, $^{13}$C NMR spectra were recorded on a Bruker AVANCE III-600 MHz and 150 MHz NMR spectrometer, respectively (Bruker, Billerica, MA). MS determinations were carried out on AB Triple TOF 5600plus System (AB SCIEX, Framingham, USA) and a LTQ-MS (Thermo) instrument. The abilities of probes reacting to $ClO^-$ in the living cells were also evaluated by using a Leica DMi8 laser scanning microscope.

*2.3. Preparation and characterization of probe **1** and probe **2***

*2.3.1. Preparation and characterization of **A***

The probes synthesis routes were using a modification of a literature method[29] and summarized in Scheme 1. A mixture of 4-bromo-1, 8-naphthalic anhydride (8.28 g, 30 mmol) and n-butylamine (2.19 g, 30 mmol) in 60 mL of ethanol was refluxed for 5 h. After the reaction was completed, the reaction mixture was evaporated in vacuum and

dried to obtain a solid product. Later on, the solid was purified by chromatography on a silica gel column in dichloromethane resulted in a pale yellow solid product **A** (8.74 g) in 88% yield. $^{1}$H NMR (DMSO-$d_6$, 600 MHz): δ (ppm): 8.53 (dd, $J$ = 7.9 Hz, 2H), 8.30 (d, $J$ = 7.6 Hz, 1H), 8.19 (d, $J$ = 7.7 Hz, 1H), 7.98 (t, $J$ = 7.8 Hz, 1H), 4.02 (t, $J$ = 7.3 Hz, 2H), 1.61 (m, 2H), 1.36 (m, 2H), 0.93 (t, $J$ = 7.4 Hz, 3H). $^{13}$C NMR (DMSO-$d_6$, 150 MHz): δ (ppm): 163.22, 163.17, 132.95, 131.94, 131.74, 131.32, 130.14, 129.51, 129.17, 128.61, 123.10, 122.32, 30.02, 20.27, 14.17. HR-MS of the compound **A**: m/z: [compound **A**+ H]$^+$ Calcd for $C_{16}H_{15}BrNO_2^+$ 332.0281, Found 332.0286 (Fig. S1).

*2.3.2. Preparation and characterization of **B***

To a 100 mL radius flask, **A** (20 mmol, 6.62 g) and sodium methoxide (20 mmol, 1.36 g) in methanol (40 mL) was refluxed for 8 h while $CuSO_4 \cdot 5H_2O$ served as catalyst. Then the crude product was evaporated in vacuum and the residue was added HCl (1 mol/L, 30 mL) to crystallize out. Subsequently, a solid separated by filtration was purified by chromatography on a silica gel column in dichloromethane to give a white product **B** (4.93 g) in 87% yield. $^{1}$H NMR (DMSO-$d_6$, 600 MHz): δ (ppm): 8.49 (d, $J$ = 8.3 Hz, 1H), 8.46 (d, $J$ = 7.2 Hz, 1H), 8.42 (d, $J$ = 8.2 Hz, 1H), 7.79 (t, $J$ = 7.8 Hz, 1H), 7.29 (d, $J$ = 8.3 Hz, 1H), 4.12 (s, 3H), 4.01 (t, $J$ = 7.4 Hz, 2H), 1.60 (m, 2H), 1.35 (d, $J$ = 14.8, 7.4 Hz, 2H), 0.93 (t, $J$ = 7.4 Hz, 3H). $^{13}$C NMR (DMSO-$d_6$, 150 MHz): δ (ppm): 163.99, 163.36, 160.74, 133.70, 131.46, 128.97, 128.66, 126.83, 123.18, 122.34, 114.69, 106.71, 57.08, 30.18, 20.29, 14.20. HR-MS of the compound **B**: m/z: [compound **B**+ H]$^+$ Calcd for $C_{17}H_{18}NO_3^+$ 284.1281, Found 284.1286 (Fig.

S2).

*2.3.3. Preparation and characterization of **C***

Compound **B** (15 mmol, 4.25 g) was added to 55% HI solution with refluxing at 140°C for 7 h, and then the mixture solution was cooled to room temperature. After that, the mixture was slowly poured into ice water, filtered and washed with distilled water. The pale yellow solid thus obtained was dried under vacuum to give compound **C** (3.75 g) in 93% yield. $^{1}$H NMR (DMSO-$d_6$, 600 MHz): δ (ppm): 11.88 (s, 1H), 8.54 (d, $J$ = 8.3 Hz, 1H), 8.48 (d, $J$ = 7.2 Hz, 1H), 8.36 (d, $J$ = 8.1 Hz, 1H), 7.77 (t, $J$ = 7.7 Hz, 1H), 7.16 (d, $J$ = 8.1 Hz, 1H), 4.02 (t, $J$ = 7.3 Hz, 2H), 1.60 (m, 2H), 1.34 (m, 2H), 0.92 (t, $J$ = 7.3 Hz, 3H). $^{13}$C NMR (DMSO-$d_6$, 150 MHz): δ (ppm): 164.13, 163.46, 160.70, 134.02, 131.59, 129.64, 129.34, 126.08, 122.84, 122.28, 113.08, 110.42, 30.22, 20.29, 14.21. HR-MS of the compound **C**: m/z: [compound **C**+ H]$^+$ Calcd for $C_{16}H_{16}NO_3^+$ 270.1125, Found 270.1136 (Fig. S3).

*2.3.4. Preparation and characterization of **D***

To a stirred 20 mL trifluoroacetic acid, **C** (10 mmol, 2.69 g) and hexamethylenetetramine (13 mmol, 1.82 g) was added, and then the mixture was refluxed at 120 ℃ for 10 h. When the remained solution was cooled to room temperature, it was slowly poured into the mixture solution of 50 mL $CHCl_3$ and 50 mL HCl (1 mol/L) and then the mixture was warmed at room temperature whilst stirring overnight. Followed that, separate the organic phase with a separatory funnel and wash the aqueous phase three times with $CHCl_3$ (20 mL×3). The merged organic layer was dried with sodium sulfate and evaporated in vacuum to dry to a solid. Then

the solid was purified by column chromatography on a silica gel (ethyl acetate: petroleum ether = 1: 3) to get a pale yellow product **D** (1.66 g) in 56% yield. $^{1}$H NMR (DMSO-$d_6$, 600 MHz): δ (ppm): 10.37 (s, 1H), 8.70 (m, 2H), 8.57 (d, *J* = 7.3 Hz, 1H), 7.87 (t, *J* = 7.8 Hz, 1H), 4.02 (t, *J* = 7.4 Hz, 2H), 1.60 (m, 2H), 1.35 (d, *J* = 14.8, 7.5 Hz, 2H), 0.93 (t, *J* = 7.4 Hz, 3H). $^{13}$C NMR (DMSO-$d_6$, 150 MHz): δ (ppm): 194.51, 165.10, 163.69, 163.02, 134.00, 133.21, 131.70, 130.50, 127.43, 124.03, 122.77, 117.59, 113.64, 30.13, 20.27, 14.20. HR-MS of the compound **D**: m/z: [compound **D**+ H]$^+$ Calcd for $C_{17}H_{16}NO_4^+$ 298.1074, Found 298.1080 (Fig. S4).

*2.3.5. Preparation and characterization of probe **1***

A mixture of **D** (0.595 g, 2 mmol), hydroxylamine hydrochloride (0.555 g, 8 mmol) and 30 μL piperidine in EtOH (25 mL) was stirred and refluxed at 80 ℃ over night. After the reaction was complete, the mixture solution was then cooled to filtered and washed with EtOH. The yellow solid thus obtained was dried under vacuum to give probe **1** (0.562 g) in 90 % yield. $^{1}$H NMR (DMSO-$d_6$, 600 MHz): δ (ppm): 12.33 (s, 1H), 11.89 (s, 1H), 8.75 (s, 1H), 8.63 (d, *J* = 8.3 Hz, 1H), 8.61 (s, 1H), 8.50 (d, *J* = 6.4 Hz, 1H), 7.84 (m, 1H), 4.05 (m, 2H), 1.61 (dt, *J* = 15.0, 7.5 Hz, 2H), 1.35 (m, 2H), 0.93 (t, *J* = 7.4 Hz, 3H). $^{13}$C NMR (DMSO-$d_6$, 150 MHz) δ (ppm): 194.51, 165.10, 163.69, 163.02, 134.00, 133.21, 131.70, 130.50, 127.43, 124.03, 122.77, 117.59, 113.64, 30.13, 20.27, 14.20. ESI-MS of the probe **1**: m/z: [Probe **1**+ H]$^+$ Calcd for $C_{17}H_{17}N_2O_4^+$ 313.12, Found 312.92 (Fig. S5).

*2.3.6. Preparation and characterization of probe **2***

A mixture of **D** (0.595 g, 2 mmol), 1,4-dimethylpyridin-1-ium iodide (0.470 g, 2

mmol) in EtOH (25 mL) was stirred and refluxed at 80 ℃ over night. After the reaction was complete, the mixture solution was cooled to filtered and washed with EtOH. The blackish green solid thus obtained was dried under vacuum to give probe **2** (0.823 g) in 80 % yield. $^{1}$H NMR (DMSO-$d_6$, 600 MHz): δ (ppm): 8.53 (d, $J$ = 6.2 Hz, 2H), 8.48 (d, $J$ = 7.2 Hz, 1H), 8.38 (s, 1H), 8.26 (d, $J$ = 7.0 Hz, 1H), 8.12 (d, $J$ = 15.4 Hz, 1H), 7.98 (d, $J$ = 6.2 Hz, 2H), 7.90 (d, $J$ = 15.3 Hz, 1H), 7.42 (t, $J$ = 7.6 Hz, 1H), 4.11 (s, 3H), 4.02 (m, 2H), 1.58 (m, 2H), 1.34 (m, 2H), 0.93 (t, $J$ = 7.3 Hz, 3H). $^{13}$C NMR (DMSO-$d_6$, 150 MHz) δ (ppm): 164.57, 163.20, 155.64, 144.11, 142.81, 142.55, 132.43, 131.97, 130.88, 123.02, 121.70, 121.53, 118.83, 116.82, 101.45, 46.30, 30.48, 20.36, 14.30. HR-MS of the probe **2**: m/z: [Probe **2**-I$^-$]$^+$ Calcd for $C_{24}H_{23}N_2O_3^+$ 387.1703, Found 387.1684 (Fig. S6).

*2.4. General UV-Vis and fluorescence spectra measurements*

All UV-Vis spectra and Fluorescence spectra were recorded using a PO-120 quartz cuvette (10 mm). Stock solutions (2 mM) of probe **1** and **2** were both prepared in 2 mL DMSO. The stock solutions of sodium hypochlorite (2 mM) were made by the mixture of 5 mL $H_2O$ and 1 mL sodium hypochlorite (13.4 mM). Other analytes including $ClO_2^-$, $ClO_3^-$, $ClO_4^-$, $F^-$, $Cl^-$, $Br^-$, $CN^-$, $SCN^-$, $MnO_4^-$, $N_3^-$, $NO_3^-$, $NO_2^-$, $CO_3^{2-}$, $AcO^-$, $P_2O_7^{4-}$, $PO_4^{3-}$, $S^{2-}$ and $HSO_3^-$ were dissolved in deionized water for the preparation of stock solutions (0.2 M). The stock solutions of $ClO^-$, $H_2O_2$ and tBuOOH were using double distilled water to dilute and $O^{2-}$ was obtained by dissolved $KO_2$ in double distilled water. tBuO· was obtained by the reactions of $H_2O_2$ and tBuOOH with ferrous perchlorate, respectively. $ONOO^-$ was obtained by the fast

mixture of $NaNO_2$, $H_2O_2$ and NaOH. In the investigated of the effect of pH on the fluorescence spectra experiment, phosphoric acid (0.5 M) and sodium hydroxide solution (0.5 M) were added sodium dihydrogen phosphate solutions (0.2 M) and sodium hydrogen phosphate solutions (0.2 M) to adjust the different pH values (2-13). The excitation wavelength of fluorescence spectra of probe **1** and **2** were 400 nm and 405 nm, respectively. And the excitation and emission slit widths of probe **1** and **2** were set to 2.5 nm and 5 nm, 5 nm and 5 nm, respectively.

*2.5. Imaging of A549 cells*

The A549 cells were grown in Dulbecco's Modified Eagle's medium supplemented with 12% Fetal Bovine Serum and 1% antibiotics at 37 ℃ in humidified environment of 5% $CO_2$. Cells were plated on 6-well plate and allowed to adhere for 24 h. Before the experiments, cells were washed with PBS three times. The A549 were treated with 2 μM probe **1** (DMSO stock solution) in culture media for 30 min at 37 ℃ and then washed with PBS three times. For the control experiment, the cells were treated with 5 mM NAC (N-acetyl-L-cysteine, it is a commonly used antioxidant) in culture media for 30 min at 37 ℃. And then, the cells were washed with PBS three times and incubated with 2 μM probe **1** in culture media for 30 min at 37 ℃. For probe **2**, the A549 were treated with 4 μM probe **2** in culture media for 30 min at 37 ℃ and then washed with PBS three times.

*2.6 Determination of quantum yield*

Fluorescence quantum yield was defined as the ratio of the number of excited molecules which were returned to the ground state by emitting fluorescence and the

total number of excited state molecules. The quantum yields were determined using quinoline sulfate ($\Phi_r$ = 0.58, 0.1 M $H_2SO_4$) as a standard reference.[30] The absorbance values of probe **1** at 400 nm of samples were less than 0.02. Accordingly, the absorbance values of probe **2** at 405 nm of samples were less than 0.02. The UV-Vis absorption and accordingly emission spectra were recorded, respectively. And then, the fluorescence quantum yield was calculated according to the formula as follow:

$$\Phi_s = \frac{\Phi_r A_r F_s}{A_s F_r}$$

Among them, the subscripts of formula r and s represent standard reference and sample, respectively.

## 3. Results and Discussions

### *3.1. UV-Vis and fluorescence spectra of detecting $ClO^-$*

To investigate the sensitivity of two probes to hypochlorite, we first made UV-Vis and fluorescence titration spectra experiments. As shown in Fig. 1a, the absorption peaks of probe **1** were at 450 nm, 372 nm and 305nm. With increasing concentration of $ClO^-$ (0-147.4 μM) in PBS (pH 7.4) containing probe **1** (4 μM), the original absorbance centered at 305 nm, 372 nm and 450 nm was gradually decreased with obvious blue-shift from 450 nm to 421 nm. Accordingly, the visible color changed from golden yellow to light green, which can be observed by the naked eye. For probe **2**, when addition of $ClO^-$ (0-1.608 mM) in PBS buffer solution (pH 7.4, containing 20% DMSO) containing probe **2** (8 μM), the original absorbance centered at 349 nm and 480 nm was gradually decreased with obvious blue-shift from 480 nm to 465 nm (Fig. 1b).

Accordingly, upon addition of $ClO^-$ (0-16 μM) in PBS (pH 7.4) containing probe **1** (2 μM), the fluorescence intensity at 515 nm ($\lambda_{ex}$ = 400 nm) increased with remarkable fluorescence color change from colorless to green (Fig. 2a) and the fluorescence quantum yield from $\Phi_{f\ probe\ 1}$ = 0.004 to $\Phi_{f\ probe\ 1\text{-}ClO^-}$ = 0.423 with quinoline sulfate as reference. As shown in Fig. 2b, the fluorescence intensity at 528 nm ($\lambda_{ex}$ = 405 nm) increased with increasing concentration of $ClO^-$ (0-589.6 μM) in PBS buffer solution (pH 7.4, containing 20% DMSO) containing probe **2** (4 μM). And fluorescence quantum yield from $\Phi_{f\ probe\ 2}$ = 0.010 to $\Phi_{f\ probe\ 2\text{-}ClO^-}$ = 0.369 with quinoline sulfate as reference. In addition, the probe **1**, probe **1**-$ClO^-$ and probe **2**, probe **2**-$ClO^-$ had excellent photostability (Fig. S7).

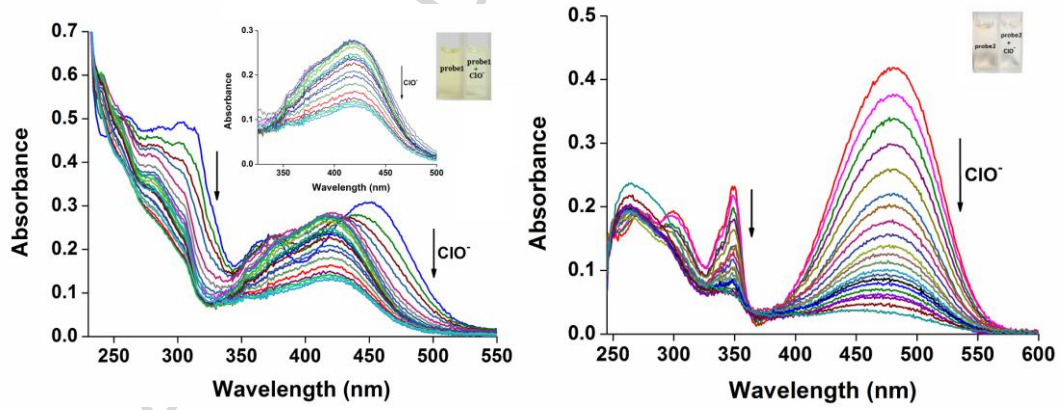


(a) (b)

**Fig. 1.** (a) The absorption spectra of the probe **1** (4 μM) in the presence of various concentrations of $ClO^-$ (0-147.4 μM) in PBS (pH 7.4); (b) The absorption spectra of the probe **2** (8 μM) in the presence of various concentrations of $ClO^-$ (0-1.608 mM) in PBS buffer solution (pH = 7.4, containing 20% DMSO).

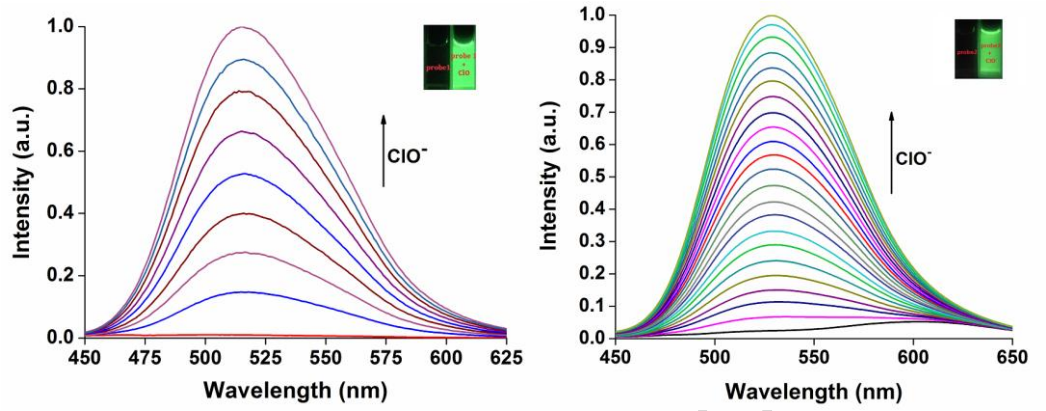


(a) (b)

**Fig. 2.** (a) Fluorescence spectra of probe **1** (2 μM) in the presence of various concentrations of $ClO^-$ (0−16 μM) in PBS (pH 7.4) ($\lambda_{ex}$ = 400 nm, $\lambda_{em}$ = 515 nm, slit: 2.5 nm/5 nm). (b) Fluorescence spectra of probe **2** (4 μM) in the presence of various concentrations of $ClO^-$ (0−589.6 μM) in PBS buffer solution (pH = 7.4, containing 20% DMSO) ($\lambda_{ex}$ = 405 nm, $\lambda_{em}$ = 528 nm, slit: 5 nm/5 nm). Inset: A visual fluorescence color change photographs for $ClO^-$ under illumination with a 365 nm UV lamp.

*3.2. The Selective response of probes to $ClO^-$*

As everyone knows, good selectivity of probe is one of the most important criteria for probe design. So, we validated the selectivity of probe **1** and **2** to hypochlorite by using UV-Vis and fluorescence spectra. Fig. S8 showed the UV-Vis spectral changes of probe **1** and **2** upon addition of various analytes including $ClO^-$, $ClO_2^-$, $ClO_3^-$, $ClO_4^-$, $H_2O_2$, $F^-$, $Cl^-$, $Br^-$, $CN^-$, $SCN^-$, $MnO_4^-$, $N_3^-$, $NO_3^-$, $NO_2^-$, $CO_3^{2-}$, $AcO^-$, $P_2O_7^{4-}$, $PO_4^{3-}$, $S^{2-}$, $HSO_3^-$, tBuOOH, tBuO•, $ONOO^-$, $O^{2-}$. As shown in Fig. S8a, only $ClO^-$ induced a decrease in the absorption peaks at 305 nm, 372 nm and 450 nm. Similarly, for probe **2**, the absorption peaks at 349 nm and 480 nm were decreased when added $ClO^-$ (Fig. S8b).

As shown in Fig. S9a, for probe **1**, a significant increase in fluorescence intensity at 515 nm was observed only in the presence of $ClO^-$ (16 μM). The other analytes (320 μM) exhibited little change on the fluorescence signal. The probe **2** (4 μM) also displayed a fluorescence enhancement when added hypochlorite (589.6 μM), while

the other analytes had no changes (Fig. S9b). In addition, selective and competitive experiments indicated that analytes including various anions and other reactive oxygen species do not disturb the determination of probe **1** and **2** for $ClO^-$ by fluorescence spectra (Fig. 3). These experiments contributed considerably to the high selectivity of the two probes for $ClO^-$.

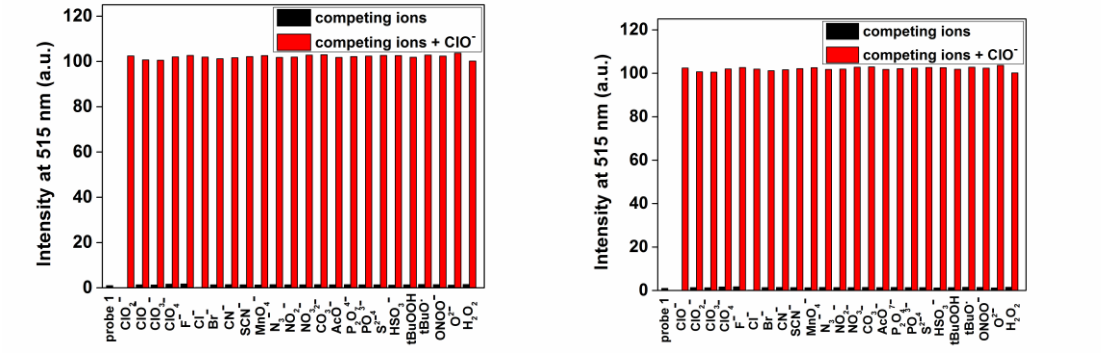


(a) (b)

**Fig. 3**. (a) Competitive binding assay responses of probe **1** (2 μM) towards various analytes (16 μM for $ClO^-$ and 320 μM for other analytes) in PBS (pH 7.4) ($\lambda_{ex}$ = 400 nm, $\lambda_{em}$ = 515 nm, slit: 2.5 nm/5 nm); (b) Competitive binding assay responses of probe **2** (4 μM) towards various analytes (589.6 μM for $ClO^-$ and 11.79 mM for other analytes) in PBS (pH 7.4) ($\lambda_{ex}$ = 405 nm, $\lambda_{em}$ = 528 nm, slit: 5 nm/5 nm).

### *3.3. Time-dependence in the detection process of $ClO^-$*

As seen from the above experiments, two probes have good sensitivity and high selectivity for $ClO^-$. In order to determine the kinetics for the reaction of the probe **1** and **2** with $ClO^-$, time-dependent fluorescence measurements were carried out. We examined the time courses of the fluorescence intensities of the probe **1** (2 μM) in the presence of $ClO^-$ (80 μM) in PBS (pH 7.4) and probe **2** (4 μM) in the presence of $ClO^-$ (589.6 μM) in PBS buffer solution (pH 7.4, containing 20% DMSO), respectively. As shown in Fig. S10, the reactions of probe **1** and **2** were complete within 50 s and 1s for $ClO^-$. It indicated that two probes reacted rapidly with $ClO^-$

under the experimental conditions.

*3.4. pH dependence*

Additionally, to evaluate the potential applications of probe in different biological environments, we studied pH effects on fluorescence intensity of two probes. From Fig. S11a, the fluorescence intensity of probe **1** appeared to be stable in the pH range 2-13 was observed for the probe **1** itself. Upon addition of $ClO^-$, the system containing probe **1** produced a distinct fluorescence increase in the pH range of 7.0-12.0. And when the solution pH was between 2.0 and 6.0 or at 13.0, $ClO^-$ induced a small fluorescence increase for probe **1**. Besides, for probe **2** (Fig. S11b), in the pH range 7-10, the fluorescence intensity of probe **2**-$ClO^-$ had distinct enhancement. As we know, HClO will decompose rapidly in strongly acidic solutions.[31] In addition, the phenolic proton of the product induced by hypochlorite is easily taken away by hydroxyl ions in alkaline solution, so the phenolic group (OH) changes into oxygen anion (O-) with rich electron cloud density and resulting in high fluorescence intensity. Therefore, the pH ranges of 7.0-12.0 and 7-10 were effective for the probe **1** and **2**, respectively. And the neutral pH was used for further studies.

*3.5 The detection limit of probes for $ClO^-$*

In addition, we investigated the detection limits of two probes for $ClO^-$. Probe **1** (2 μM) was treated with various concentrations of $ClO^-$ (0-16 μM) and the fluorescence intensity of probe at 515 nm was plotted as a function of the $ClO^-$ concentration. Also, probe **2** (4 μM) was treated with various concentrations of $ClO^-$ (0-589.6 μM) and the fluorescence intensity of probe at 528 nm was plotted as a function of the $ClO^-$

concentration. We used the equation ($C_{DL}$ = 3 $S_b$/m) based on the definition by IUPAC to calculate the detection limit, where $S_b$ is the standard deviation of blank measurements, m is the slope of the plot of the fluorescence intensity as a function of the concentrations of $ClO^-$. Through calculation, the detection limits of probe **1** and **2** were found to be 2.882 nM and 0.354 μM (Fig. 4). The experiments showed that the detection limit of probe **1** was much lower than the probe **2**. Compared with other reported $ClO^-$ probes, two probes showed a high sensitivity towards $ClO^-$ (Table S1). [32-36]

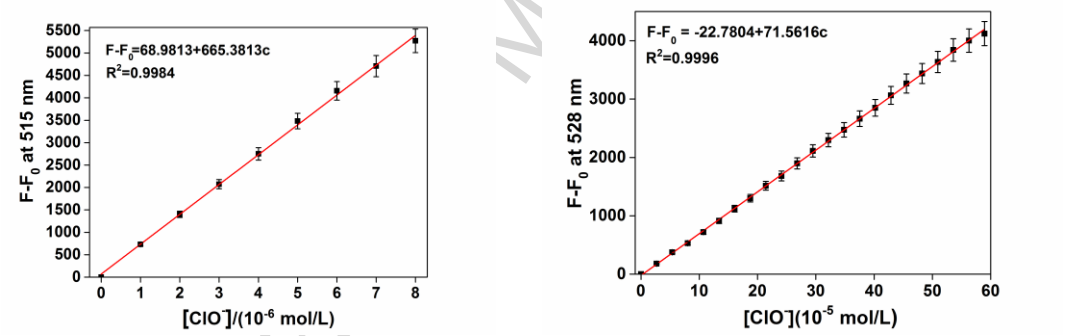


(a) (b)

**Fig. 4.** (a) Plot of the fluorescence intensity of probe **1** at 515 nm as a function of the concentration of $ClO^-$ ($\lambda_{ex}$ = 400 nm). (b) Plot of the fluorescence intensity of probe **2** at 528 nm as a function of the concentrations of $ClO^-$ ($\lambda_{ex}$ = 405 nm).

*3.6 Theoretical calculation*

In order to further study the optical properties, molecular calculations for probe **1** and **2** and their oxidation products probe **1**-$ClO^-$ and probe **2**-$ClO^-$ have been calculated by the Gaussian 09 program package.[37] The ground state geometries and electron structures of the complexes were optimized by means of the density functional theory (DFT) method at the b3lyp/6-31+G (d, p) level and the solvent was water. As shown in Table S2a, the DFT calculation confirmed that the allowed S0-S1

electronic transitions with oscillator strength f=0.68634 and 0.68849 were identified as the allowable transitions of the probe **1** and probe **1**-$ClO^-$, which were composed of HOMO→LUMO and HOMO→LUMO transitions, respectively. The electronic cloud of HOMO for the probe **1** was dispersed inside the whole molecular framework and the LUMO for the probe **1** was locally distributed inside the 6-hydroxy-1H-benzo[de]isoquinoline-1,3(2H)-dione group (Fig. 5a). However, the electronic cloud of probe **1**-$ClO^-$ both the HOMO and LUMO were dispersed inside the whole molecular framework. It showed that the fluorogenic process was mainly mediated by the intramolecular charge transfer (ICT) mechanism. The ICT process can take place in probe **1**, which resulted in weaker fluorescence emissions. Accordingly, in probe **1**-$ClO^-$, ICT process was prohibited and therefore a stronger fluorescence was observed.

As shown in Table S2b, the DFT calculation confirmed that the allowed S0-S1 electronic transitions with oscillator strength f=0.0350 and 0.3700 were identified as the allowable transitions of the probe **2** and probe **2**-$ClO^-$, which were composed of HOMO→LUMO and HOMO→LUMO, HOMO→LUMO+1 transitions, respectively. The electronic cloud of HOMO for the probe **2** was locally concentrated inside the C=C, which was connected with 1, 4-dimethylpyridin-1-ium iodide and 1, 8-naphthalimide group (Fig. 5b). Besides, the electronic cloud of LUMO for the probe **2** was dispersed inside the whole molecular framework. For the electronic cloud of probe **2**-$ClO^-$, both the HOMO and LUMO were dispersed inside the whole molecular framework. It also showed that the fluorogenic process was mainly

mediated by the intramolecular charge transfer (ICT) mechanism. On the basis of theoretical calculation, the optical properties of probe **1**, probe **1**-$ClO^-$ and probe **2**, probe **2**-$ClO^-$ have been theoretically revealed.

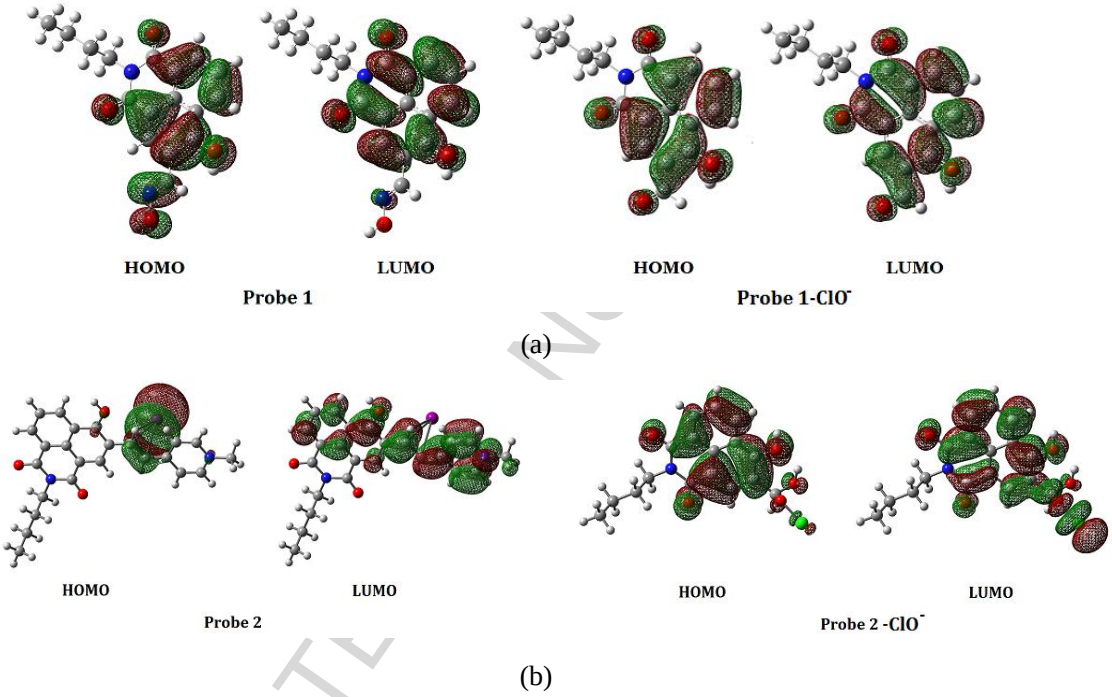


**Fig. 5.** The frontier molecular orbitals of (a) probe **1**, probe **1**-$ClO^-$ and (b) probe **2**, probe **2**-$ClO^-$ theoretically predicted at B3LYP/6-31+G (d, p) level.

*3.7. Proposed mechanism*

To explore the sensing mechanism, mass spectrometry analyses and NMR spectroscopic analyses were studied. For probe **1**, mass spectrometry analysis of a product obtained from the reaction of probe **1** with $ClO^-$ in $CH_3OH$ supported the formation of probe **1**-$ClO^-$ compound. A peak at 297.82 corresponding to [Probe **1**-$ClO^-$ + H]$^+$ was clearly observed (Fig. S12a). Further NMR spectroscopic analysis also provided the evidence that hypochlorite can oxidate oxime structure (-C=N-OH) of probe **1** for aldehyde group. From Fig. S12b, the peak at 11.87 ppm, which was assigned to oxime ($CH_{-C=N-OH}$) of probe **1**, with addition of hypochlorite, the peak at 11.87 ppm was gradual disappeared and a new peak at 10.17 was appeared. And the

peak of hydroxyl ($CH_{\text{-CHO}}$) was displaced from 12.35 ppm to 10.42 ppm. Nuclear magnetic titration experiment and mass spectrum datum proved that the mechanism of probe **1** with hypochlorite was hypochlorite can oxidate oxime group into aldehyde group (Fig. 6a).

Mass spectrometry analysis of a product obtained from the reaction of probe **2** with $ClO^-$ in $CH_3OH$ supported the formation of probe **2**-$ClO^-$ compound. A peak at 350.0748 corresponding to [Probe **2**-$ClO^-$ + H]$^+$ was clearly observed (Fig. S13a) and a peak at 352.0725 was the chlorine isotope peak of [Probe **2**-$ClO^-$ + H]$^+$. We tried our best to isolate the product induced by hypochlorite many times, but always failed. So we just carried out NMR titration experiments, namely we directly added sodium hypochlorite solution into DMSO-$d_6$ including probe 2, as shown in Fig. S13b, $^1$HNMR showed that the number of aromatic hydrogens obviously decreased after addition of hypochlorite. It implied that probe 2 was oxidized by hypochlorite, resulting in the pyridine ring leaving. However, after long time scaning, $^{13}$CNMR could not give any information.

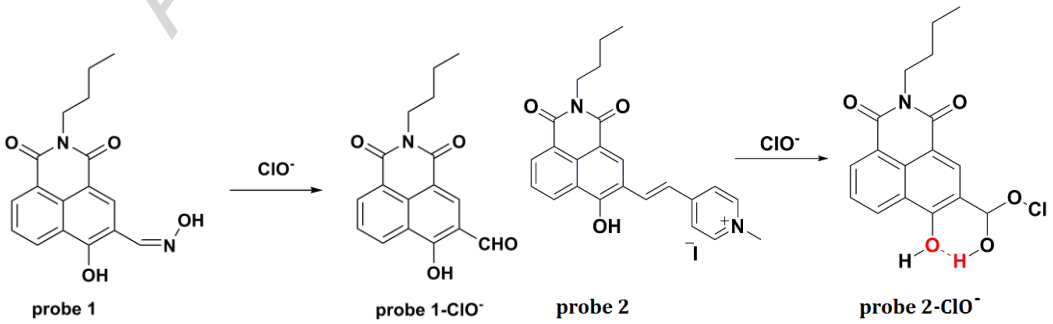


(a) (b)

**Fig. 6.** The possible mechanism of porbe **1** (a) and probe **2** (b) with $ClO^-$.

*3.8. Cellular Imaging*

We further investigated the fluorescence imaging of two probes (Fig. 7). The A549

cells were treated with 4 μM probe **2** in culture media for 30 min at 37 ℃ showed no light (Fig. 7A). On the contrary, the same cells were treated with 2 μM probe **1** in culture media for 30 min at 37 ℃ shown distinct green (Fig. 7D). For the control experiment, the cells were first treated with 5 mM NAC (N-acetyl-L-cysteine) in culture media for 1 h at 37 ℃ and then incubated with 2 μM probe **1** in culture media for 30 min at 37 ℃ showed no light (Fig. 7G). The latter two experiments showed that probe **1** can detect intracellular hypochlorite. And cellular imaging experiments also indicated that probe **1** has higher sensitivity for hypochlorite than probe **2**.

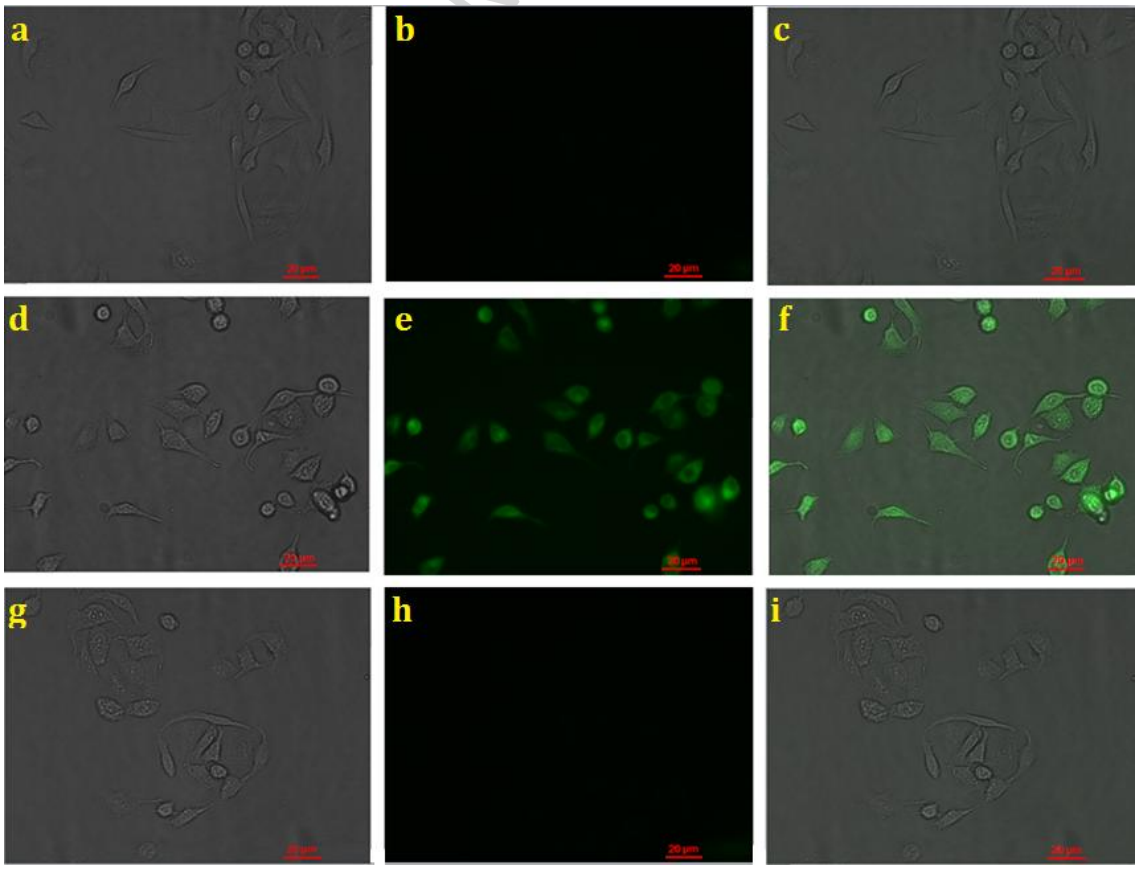


**Fig. 7.** Fluorescence and bright field images of A549 cells. (a) Fluorescence image of cells incubated with probe **2** (4 μM) for 30 min and its bright field image (b), merged image (c). (d) A549 cells were treated with probe **1** (2 μM) and its bright field image (e), merged image (f). (g) Fluorescence image of cells pre-treated with NAC (5 mM) for 30 min and then incubated with probe **1** (2 μM) for 30 min. (h) Bright-field image of g. (i) Merged image of g and h.

*3.9 Detection of $ClO^-$ in water samples*

To take advantage of their good spectroscopic responses of hypochlorite, two probes were applied to detect the hypochlorite concentration of tap water and river water. Tap water and river water were obtained from Shanxi University. The analysis results of two probes were shown in Table 1. From Table 1, the values of recovery were showed from 99.20 % to 102.00 % in tap water and from 98.60 % to 99.50 % in river water of probe **1**, and the values of recovery were showed from 97.41 % to 99.79 % in tap water and from 95.67 % to100.98 % in river water of probe **2**. The experimental results suggested that both probe **1** and **2** were promising fluorescence probes for the detection of hypochlorite in water samples.

| Probe | Sample | $ClO^-$ spiked (M) | Found (M) mean±SD | Recovery (%) |
|---|---|---|---|---|
| **1** | Tap water 1 | $5\times10^{-6}$ | $(13.05\pm0.02)\times10^{-6}$ | 99.20 |
| | Tap water 2 | $8\times10^{-6}$ | $(26.39\pm0.04)\times10^{-6}$ | 102.00 |
| | Tap water 3 | $10\times10^{-6}$ | $(33.43\pm0.01)\times10^{-6}$ | 100.90 |
| | River water 1 | $5\times10^{-6}$ | $(13.21\pm0.02)\times10^{-6}$ | 99.01 |
| | River water 2 | $8\times10^{-6}$ | $(37.16\pm0.01)\times10^{-6}$ | 99.50 |
| | River water 3 | $10\times10^{-6}$ | $(32.05\pm0.03)\times10^{-6}$ | 98.60 |
| **2** | Tap water 1 | $13.4\times10^{-5}$ | $(4.95\pm0.03)\times10^{-5}$ | 97.41 |
| | Tap water 2 | $26.8\times10^{-5}$ | $(8.16\pm0.02)\times10^{-5}$ | 98.62 |
| | Tap water 3 | $33.5\times10^{-5}$ | $(10.09\pm0.05)\times10^{-5}$ | 99.79 |
| | River water 1 | $13.4\times10^{-5}$ | $(4.95\pm0.04)\times10^{-5}$ | 98.58 |
| | River water 2 | $26.8\times10^{-5}$ | $(7.96\pm0.03)\times10^{-5}$ | 100.98 |
| | River water 3 | $33.5\times10^{-5}$ | $(9.86\pm0.06)\times10^{-5}$ | 95.67 |

**Table 1** The testing results of $ClO^-$ concentration in tap water and river water samples.

## 4. Conclusion

In a word, two novel 1, 8-naphthalimide-based turn-on fluorescent probes were devised and developed by utilizing the oxidation of hypochlorite. Probe **1** and **2** displayed rapid and remarkable turn-on responses to $ClO^-$ in PBS buffer solution (pH

7.4) and PBS buffer solution (pH = 7.4, containing 20% DMSO). Furthermore, the detection limits of probe **1** and **2** for $ClO^-$ were as low as 2.882 nM and 0.354 μM. In addition, the detailed signal mechanisms were carried out by MS and NMR spectroscopic methods. More importantly, fluorescence imaging experiments demonstrated that probe **1** can be more suitable for detecting the endogenous $ClO^-$ in living A549 cells. And both two probes had the possibility of potentially applied in practical applications such as detecting the hypochlorite concentration of tap water and river water.

**Acknowledgments**

We thank the National Natural Science Foundation of China (No. 21472118, 21672131), the Program for the Top Young and Middle-aged Innovative Talents of Higher Learning Institutions of Shanxi (2013802), Talents Support Program of Shanxi Province (2014401), Shanxi province Outstanding Youth Fund (2014021002).

**References**

[1] X. Q. Chen, X. Z. Tian, I. Shin and J. Yoon, Chem. Soc. Rev., 40 (2011) 4783-4804.

[2] B. D'Autreaux and M. B. Toledano, Nat. Rev. Mol. Cell Biol. 8 (2007) 813-824.

[3] K. H. Xu , L. L. Wang , M. M. Qiang , L. Y. Wang , P. Li and B. Tang, Chem. Commun., 47 (2011) 7386-7388.

[4] M. Valko, D. Leibfritz, J. Moncol, M. T. D. Cronin, M. Mazur and J. Telser, Int. J. Biochem. Cell Biol. 39 (2007) 44-84.

[5] M. S. Shim and Y. N. Xia, Angew. Chem. Int. Ed., 52 (2013) 6926-6929.

[6] Y. B. Ding, Y. Y. Tang, W. H. Zhu and Y. X. Xie, Chem. Soc. Rev., 44 (2015) 1101-1112.

[7] X. M. Wang, X. H. Wang, Y. Feng, M. Z. Zhu, H. Yin, Q. X. Guo and X. M. Meng, Dalton Trans., 44 (2015) 6613-6619.

[8] J. Kim and Y. Kim, Analyst, 139 (2014) 2986-2989.

[9] S. Goswami and S. Paul, Dalton Trans., 42 (2013) 10097-10101.

[10] Y. B. Ding, X. Li, T. Li, W.H. Zhu and Y.S. Xie, J. Org. Chem., 78 (2013) 5328-5338.

[11] G. P. Li, D. J. Zhu, Q. Liu, L. Xue and H. Jiang, Org. Lett., 15 (2013) 2002-2005.

[12] L. Yuan, W. Y. Lin, J. Z. Song and Y. T. Yang, Chem. Commun., 47 (2011) 12691-12693.

[13] G. Y. Li, Q. Lin, L. N. Ji and H. Chao, J. Mater. Chem. B, 2 (2014) 7918-7926.

[14] Q. A. Best, N. Sattenapally, D. J. Dyer, C. N. Scott and M. E. McCarroll, J. Am. Chem. Soc., 135 (2013) 13365-13370.

[15] H. J. Lee, M. J. Cho and S. K. Chang, Inorg. Chem., 54 (2015) 8644 -8649.

[16] B. Chen, Y. B. Ding, X, Li, W. H. Zhu, J. P. Hill, K. Ariga and Y. S. Xie, Chem. Commun., 49 (2013) 10136-10138.

[17] Y. B. Ding, W. H. Zhu and Y. S. Xie, Development of Ion Chemosensors Based on Porphyrin Analogues. Chem. Rev., DOI: 10.1021/acs.chemrev.6b00021.

[18] Q. Wang, C. Liu, J. J. Chang, Y. Lu, S. He, L. C. Zhao and X. S. Zeng, Dyes and Pigments, 99 (2013) 733-739.

[19] W. Lin, L. Long, B. Chen and W. Tan, Chem. Eur. J. 15 (2009) 2305-2309.

[20] Z. Tang, X. L. Ding, Y. Liu, Z. M. Zhao and B. X. Zhao, RSC Adv., 5 (2015) 99664-99668.

[21] J. T. Hou, K. Li, J. Yang, K. K. Yu, Y. X. Liao, Y. Z. Ran, Y. H. Liu, X. D. Zhou and X. Q. Yu, Chem. Commun., 51 (2015) 6781-6784.

[22] L. L. Long, D. D. Zhang, X. F. Li, J. F. Zhang, C. Zhang and L. P. Zhou, Anal. Chim. Acta, 775 (2013) 100-105.

[23] J. J. Hu, N. K. Wong, M. Y. Lu, X. M. Chen, S. Ye, A. Q. Zhao, P. Gao, R. Y. Kao, J. G. Shen and D. Yang, Chem. Sci., 7 (2016) 2094-2099.

[24] X. H. Cheng, R. L. Tang, H. Z. Jia, J. Feng, J. G. Qin and Z. Li, ACS Appl. Mater. Interfaces, 4 (2012) 4387-4392.

[25] X. H. Lu, W. Wang, Q. Dong, X. L. Bao, X. F. Lin, W. X. Zhang, X. C. Dong and W. L. Zhao, Chem. Commun., 51 (2015) 1498-1501.

[26] Y. L. Pak, J. Li, K. C. Ko, G. Kim, J. Y. Lee and J. Yoon, Anal. Chem., 88 (2016) 5476-5481.

[27] M. M. Salim, E. A. Owens, T. Gao, J. H. Lee, H. Hyun, H. S. Choi and M. Henary, Analyst, 139 (2014) 4862-4873.

[28] S. Y. Lim, K. H. Hong, D. I. Kim, H. Kwon and H. J. Kim, J. Am. Chem. Soc., 136 (2014) 7018-7025.

[29] J. F. Li, P. F. Li, F. J. Huo, C. X. Yin, T. Liu, J. B. Chao and Y. B. Zhang, Dyes and Pigments, 130 (2016) 209-215.

[30] W. F. Niu, L. Guo, Y. H. Li, S. M. Shuang, C. Dong and M. S. Wong, Anal. Chem., 88 (2016) 1908-1914.

[31] Y.K. Yue, C.X. Yin, F.J. Huo, J.B. Chao and Y.B. Zhang. Sens. Actuators, B 202 (2014) 551-556.

[32] H. Zhu, J. L. Fan, J. Y. Wang, H. Y. Mu and X. J. Peng, J. Am. Chem. Soc., 136 (2014) 12820-12823.

[33] W. C. Chen, P. Venkatesan and S. P. Wu, Anal. Chim. Acta, 882 (2015) 68-75.

[34] Y. Zhou, J. Y. Li, K. H. Chu, K. Liu, C. Yao and J. Y. Li, Chem. Commun., 48 (2012) 4677-4679.

[35] G. F. Wu, F. Zeng and S. Z. Wu, Anal. Methods, 5 (2013) 5589-5596.

[36] L. J. Liang, C. Liu, X. J. Jiao, L. C. Zhao and X. S. Zeng, Chem. Commun., 52 (2016) 7982-7985.

[37] Y. T. Yang, F. J. Huo, C. X. Yin, A. M. Zheng, J. B. Chao, Y. Q. Li, Z. X. Nie and R. Martínez-Máñez, D. S. Liu, Biosens. Bioelectron., 47 (2013) 300-306.

## Abstract Graphic

# The statement:

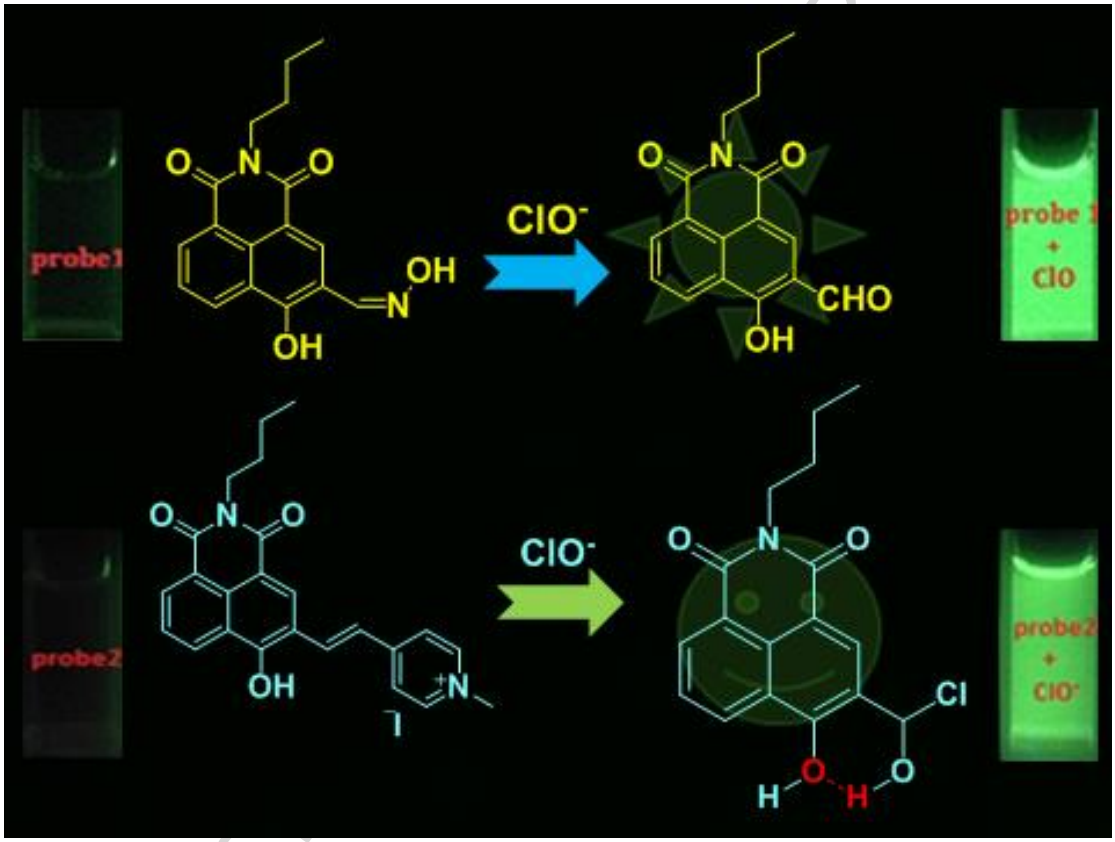


In this study, two efficient turn-on fluorescent probes based on 1, 8-Naphthalimide for hypochlorite have been rationally devised and constructed. The detection limits of probe **1** and **2** for $ClO^-$ were calculated for 2.882 nM and 0.354 μM. Moreover, the optical properties of two probes and their $ClO^-$-addition products were confirmed by density functional theory calculations. And both two probes had the possibility of potentially applied in practical applications such as detecting the hypochlorite concentration of tap water and river water.

# Highlight

1. Two probes based on 1, 8-Naphthalimide had excellent sensitivity and high selectivity for the detection of $ClO^-$.
2. The recognition mechanisms of the two probes were studied and their optical properties were confirmed by density functional theory calculations.
3. Two probes in practical application was demonstrated